

1 **Evaluation of Atmospheric Conditions Leading to a Fumigation Event**2 *Brian Viner, Steve Weinbeck, Christopher Sobecki*3 *Savannah River National Laboratory*4 *Savannah River Site*5 *Aiken, SC 29808*

6

7 **Abstract**8 During the afternoon of January 30, 2022, the Savannah River Site experienced unusual temperature
9 conditions leading to a fumigation event that triggered safety alarms and caused considerable confusion
10 about the cause of the event. Normally, it is assumed that fumigation events occur early in the day once
11 surface heating has begun. While most fumigation events are related to the break-up of a nocturnal
12 inversion, this event was related to synoptic atmospheric conditions which provided a more unique
13 scenario that led to the fumigation event. The unusual synoptic atmospheric conditions led to the
14 downwash and fumigation of the elevated plume causing a pollutant to mix rapidly to the surface. These
15 conditions could have potentially harmed workers within the facility since the plume was directed toward
16 a building air intake system. We seek to outline the conditions that led to this unusual fumigation event
17 and provide results of 2-D wind modeling of the event to characterize these conditions for future
18 operational guidance of the facility air intake systems. This work sets the groundwork for future, high-
19 resolution modeling to explore the mechanisms and thresholds affecting fumigation on the facility-
20 specific short distance scales and improve forecasting of non-standard fumigation events to protect
21 human health.

22

23 **Keywords:** Fumigation; Building Downwash; CFD Modeling; Atmospheric Dispersion

24 **Introduction**

25 Fate and transport evaluation of airborne plumes is a key component of facility safety basis modeling
26 used to ensure the health and safety of co-located workers and downwind individuals. Downwind
27 dispersion is the primary mode of plume travel that is considered, but special cases such as fumigation
28 and aerodynamic downwash must also be considered as significant factors impacting plume travel
29 (Bierly and Hewson 1962). These can lead to impacts beyond what plume models typically account for.
30 These additional factors can act to increase the expected surface concentration, creating a risk for
31 harmful plume constituents to enter through building air intakes, potentially exposing interior workers
32 who may be expected to have some measure of protection, and disrupting facility operations.

33 Atmospheric conditions at the Savannah River Site (SRS) near Aiken, SC may have caused a fumigation
34 event on January 30, 2022, prompting investigation into the atmospheric conditions contributing to the
35 event and whether better understanding of the conditions could lead to improved weather forecasts
36 and have operational procedures to respond to future events.

37 Atmospheric temperature inversions form from a variety of different conditions including nocturnal
38 cooling at ground level; warm air flowing over a large body of cold water; subsidence inversion caused by
39 adiabatic compression in the mid-troposphere; differential warm air advection; and frontal inversion. At
40 the SRS, inversions typically occur due to nocturnal cooling. The remaining atmospheric phenomena
41 associated with temperature inversions are infrequent regional scale phenomena that occur over and
42 across multiple states concurrently. Within this regional scale phenomena, the set of conditions that could
43 lead to a fumigation event occur much less frequently.

44 Inversions are important to understanding the effects of atmospheric dispersion, because when they
45 occur, plumes are restricted in their ability to disperse or dilute. Dispersion in the layer underneath the
46 inversion is limited by stable (negatively buoyant) air which suppresses turbulence that would otherwise
47 disperse the plume through mixing. Stable conditions at night under an inversion with low wind speed are
48 considered the most restrictive dispersion conditions. Most inversions are caused by nocturnal cooling at
49 the ground and form as outgoing longwave radiation is emitted upward from the surface at night. These
50 situations are the basis of many fumigation event studies and early modeling work (Segal and Pielke,
51 1983). Nocturnal inversions tend to be shallow, typically on the order of 100-200 m, and subsequently,
52 once the sun rises, a combination of turbulent mixing and daytime heating will quickly mix out the
53 inversion and the plume becomes less concentrated.

54 Recent work related to fumigation and mixing of plumes to the surface are generally focused on emissions
55 of greenhouse gases or pollutants in urban areas where these can pose a threat to human health (Mushtaq
56 et al. 2020; Hossain 2023). In most cases, it is acknowledged that the key considerations are related to
57 development or break-up of a low-level atmospheric temperature inversion and that the key predictors
58 of a fumigation event are generally low wind speeds and a lack of (or a cap on) thermal buoyancy in the
59 atmosphere.

60 While work related to the fumigation of plumes in industrial settings is important, little work is being
61 done with this setting in mind. As a result, many industrial applications of fumigation prediction and
62 modeling are still based on decades-old work. Most advancements in this area are related to improving

63 existing models (Warren et al. 2022) or developing machine-learning or other advanced computing
 64 techniques to assess these situations (Feng et al. 2020).

65 This paper examines the atmospheric conditions that are believed to have led to the potential
 66 recirculation event and leverages high-resolution computational fluid dynamic modeling to identify
 67 whether re-circulation of an elevated plume to the surface may have occurred in the vicinity of the release
 68 stack. This event is somewhat unique in that the occurrence of a nocturnal inversion was not solely the
 69 cause of the event, as the fumigation event occurred in mid-afternoon, well after sunrise. This work seeks
 70 to outline the synoptic meteorological conditions that contributed to the timing of the event and
 71 demonstrate an example of a high-resolution 2-D model, which can provide a basis for future work to
 72 explore the frequency and industrial hazards associated with re-circulating plumes.

73

74 **Methods**

75 *Analysis of Atmospheric Conditions*

76 The fumigation event being analyzed in this study occurred on January 30th, 2022. The event was
 77 identified in an area of a Tritium processing facility which consists of single-story process buildings with
 78 the plume being emitted from a 30 m stack located near the center of the facility. Based on
 79 measurements at the stack, a release of tritium occurred from the facility at approximately 14:30 LST
 80 and lasting for approximately five minutes. Following the release, there were indications that the plume
 81 mixed to the surface where it would have had the potential to be taken into the facility through building
 82 air intakes within 200 m of the facility and expose individuals inside the facility.

83 Given the timing of the event as occurring mid-afternoon, this event was not related to a nocturnal
 84 surface inversion resulting from nighttime cooling. As such, analysis of the event requires an
 85 examination of regional and synoptic-scale weather patterns. This data was obtained from the National
 86 Oceanic and Atmospheric Administration (NOAA) using archived synoptic maps of surface and upper air

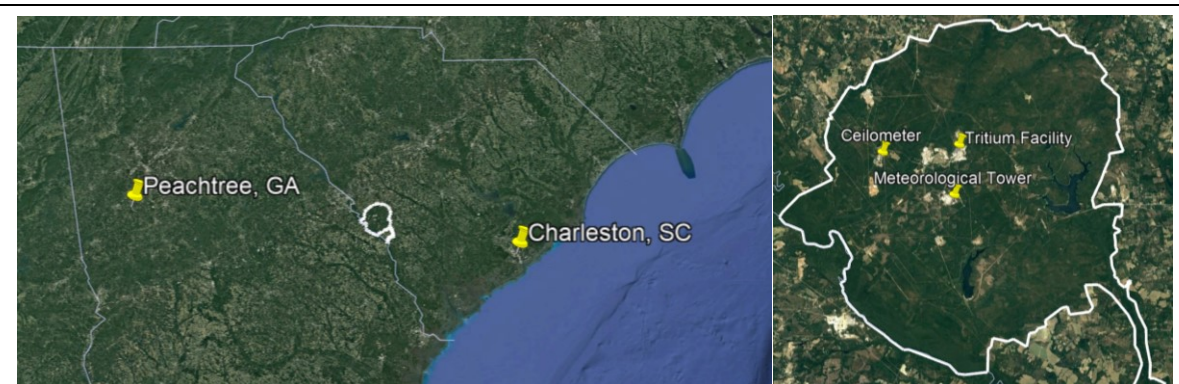


Figure 1: Map of measurement sites, including: Locations of the Savannah River Site (outlined in white) and regional atmospheric sounding sites at Peachtree City, GA and Charleston, SC (left); Instrumentation sites at the Savannah River Site including the ceilometer, meteorological measurement tower, and tritium facility location (right).

87 conditions at 925mb and 850mb which were available from www.wpc.ncep.noaa.gov and
 88 www.spc.noaa.gov, respectively. Archived upper-air soundings from two nearby sounding sites were
 89 also obtained from <http://www.weather.uwyo.edu> to aid in characterization of the regional
 90 atmospheric conditions.

91 Additional data was obtained from the meteorological monitoring network maintained at the SRS
 92 (Figure 1). For this analysis, data from a tower located 4.7 km to the south of the impacted facility was
 93 used. This tower is instrumented with RM Young Temperature/Relative Humidity Probes (Model
 94 41382V) mounted in Model 43502 aspirated radiation shield. RM Young Sonic Anemometers (Model
 95 81000) are used to provide temperature and 3-D wind measurements at 18 m, near the level of the
 96 stack. Additionally, a Vaisala CL 31 ceilometer is located at the SRS which can be used to provide
 97 information regarding boundary layer development leading up to the event. Details of the
 98 meteorological monitoring program and data quality assurance procedures are detailed in (Weinbeck,
 99 et. al. 2020).

100

101 *Fluent Modeling*

102 To simulate the event at the SRS, a numerical analysis was carried out to visualize the wind profile
 103 around the stack and nearby buildings by simultaneously solving the continuity, momentum, and energy
 104 equations, along with the turbulence models represented by the standard k-epsilon using the
 105 computational fluid dynamic simulation software ANSYS FLUENT 2021 R1. The air is treated as a
 106 continuum by solving the Navier-Stokes and energy equations. As seen in Figure 2, a numerical domain

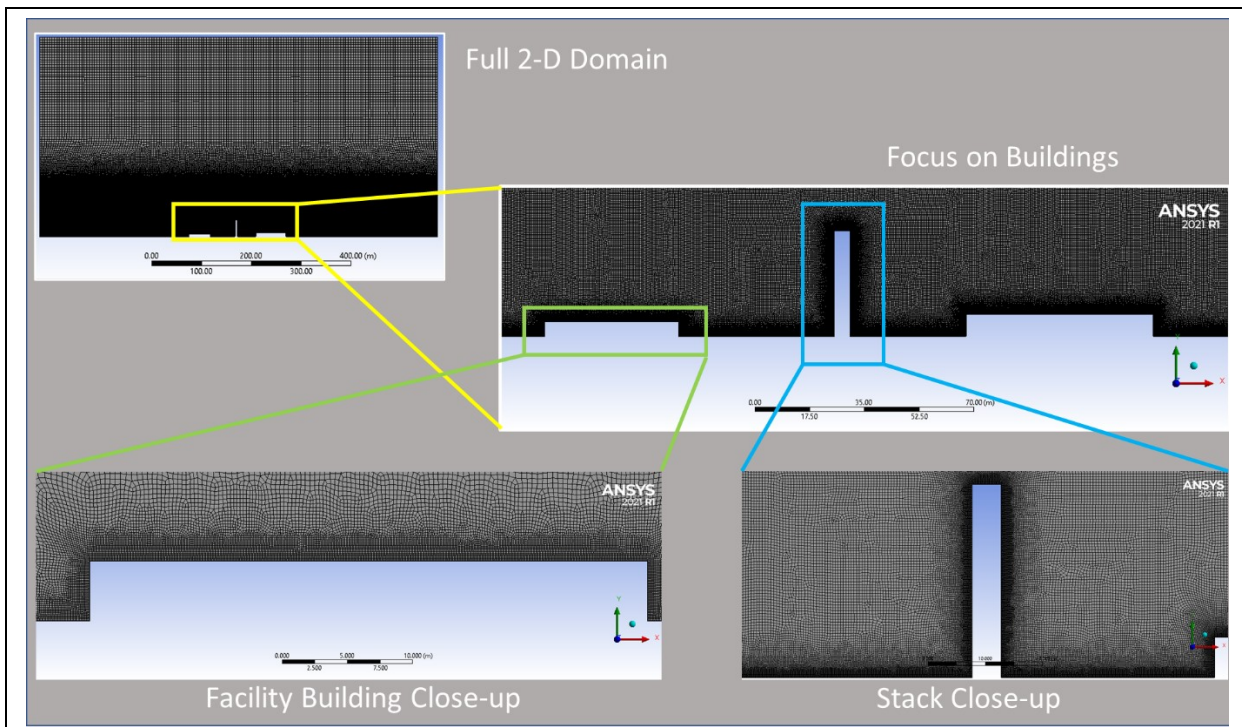


Figure 2. Illustration of the meshes used to simulate flow the release stack and nearby facilities.

107 having a length and height of 800 m and 400 m, respectively, is constructed in a 2-D rectangular shape.
 108 The velocity inlet and pressure outlet boundary conditions are implemented on the left and right side of
 109 the domain, respectively, whereas a no-slip boundary condition, with a zero-roughness height, is applied
 110 to the ground, walls and roof of the buildings, and sides and top of the stack. Finally, a symmetry
 111 boundary condition is applied at the top of the domain to reduce the backflow and improve the
 112 convergence of the computation while ensuring that the symmetry boundary condition is sufficiently far
 113 away from the buildings so that the wind velocity profile near the area of interest would not be affected.
 114 The buildings mimicking the air blockage are placed far away from the inlet for a fully developed velocity
 115 profile. The left building has a height and length of 4.57 m and 42.67 m, respectively, and is placed 300
 116 m away from the domain inlet. The stack height and outlet diameter are 33.50 m and 5.00 m,
 117 respectively, and is placed 49.78 m from the left building. The building on the right portion of the
 118 domain has a height and length of 7.01 m and 59.83 m, respectively, and is placed 37.13 m away from
 119 the stack and about 305 m from the domain outlet. For meshing, the lower part of the domain was
 120 meshed finer than the top part of the domain to observe the downwash near the buildings and for
 121 computational time. The total number of elements is 532642.
 122 The domain of the model is imported into Fluent with the standard k-epsilon equation solving the
 123 turbulence model along with the energy equation. The solution includes a gravitational force and
 124 assumes steady state. The wind speed profile at the atmospheric inlet velocity is given by the power law:

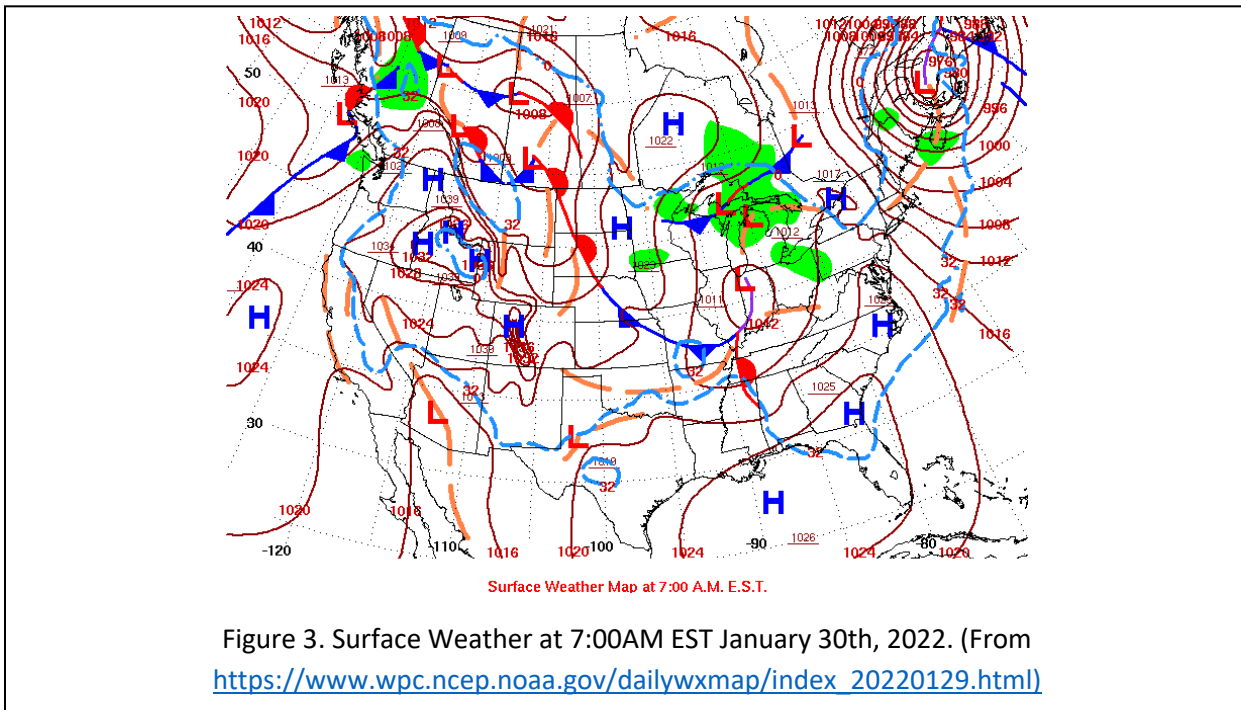
$$125 \quad U = U_{ref} \left(\frac{y}{y_{ref}} \right)^\alpha, \quad (1)$$

126 where, U_{ref} , is the reference velocity at 3 m/s, y , is the node/cell position in the computational domain,
 127 y_{ref} , is the reference height at 18 m, and α is the coefficient of the power law. The temperature of the
 128 domain remains uniform at 283.15 K, and outlet boundary condition was kept as a static pressure outlet.
 129 The simulation involved a coupled pressure-velocity solving method, with a least square cell-based
 130 solution method. The pressure, momentum, turbulent kinetic energy, turbulent dissipation rate, and
 131 energy equations were solved as second order solutions.
 132

133 **Results and Discussion**

134 *January 30th, 2022 Fumigation Event Analysis*

135 On January 29th, 2022, a strong frontal system moved through the Southeast United States. In the wake
 136 of the frontal passage, a surface cold airmass moved through South Carolina, illustrated by the 0°C
 137 isotherm south of SRS in Georgia and Florida (light blue dashed line in Figure 3), indicating temperatures
 138 in South Carolina were below freezing. Simultaneously, warm air advection was occurring at the 925 and
 139 850mb levels, creating a thermal inversion across Florida, Georgia, South Carolina and North Carolina
 140 (Figures 4 and 5), illustrated by the wind blowing from warmer air (thicker 500mb heights) to cooler air
 141 (shallower 500mb heights) over the Georgia and South Carolina region. Also of importance is that a
 142 surface high pressure system covered most of the region, providing clear skies allowing for strong
 143 surface heating on January 30th, 2022.



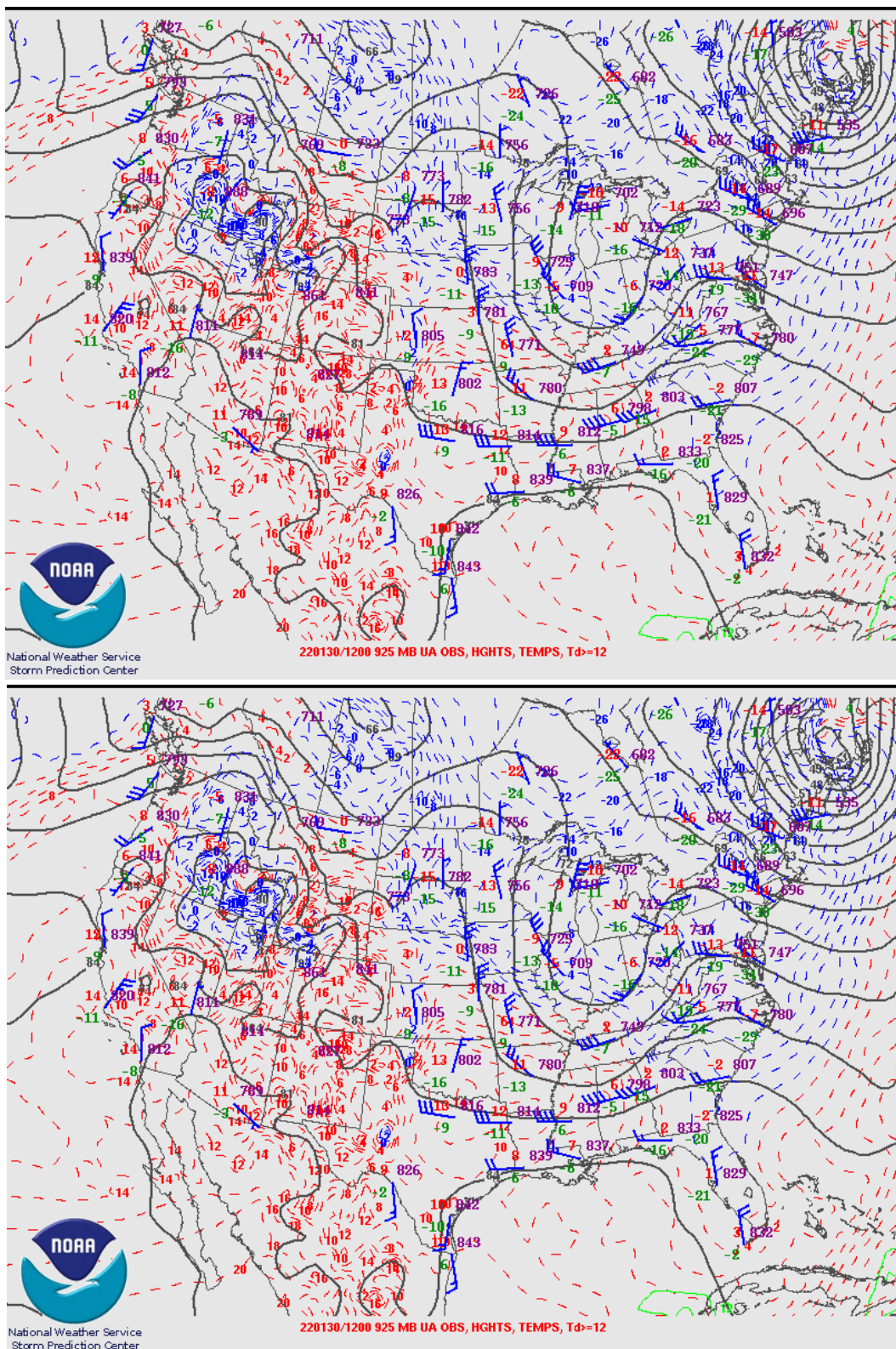


Figure 4. 925 mb analysis for 7 AM Jan 30th (top), and 7 PM Jan 31st, 2022. Images obtained from <https://www.spc.noaa.gov/obswx/maps/>.

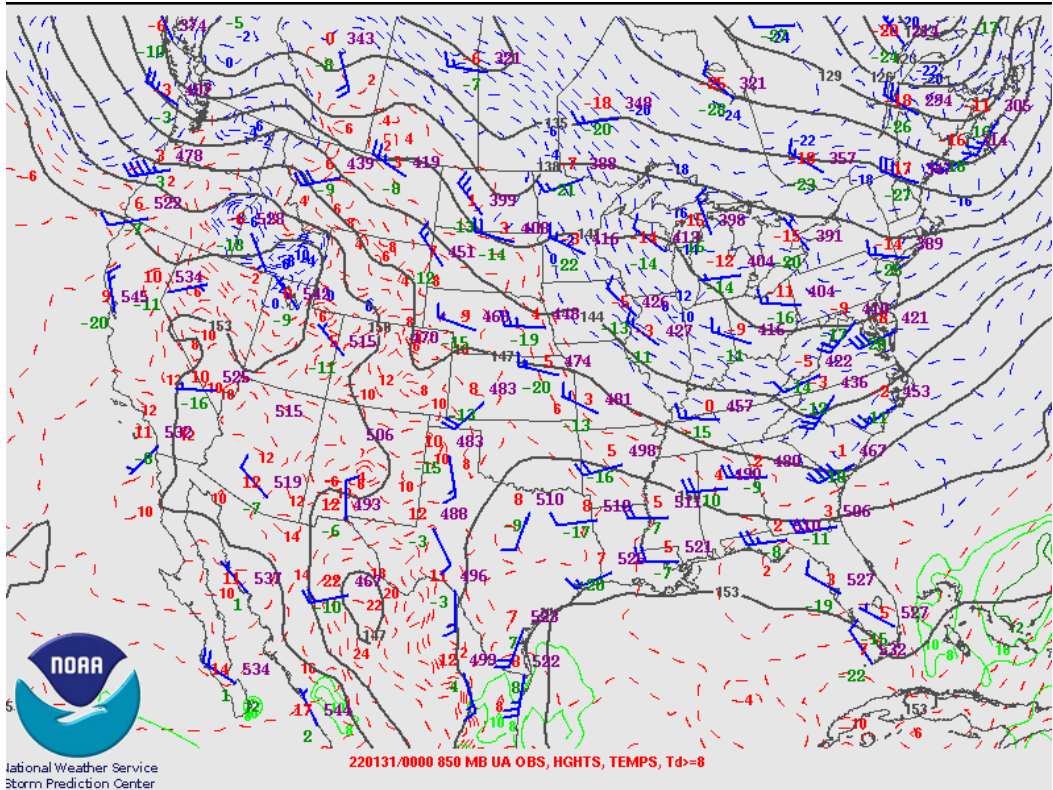
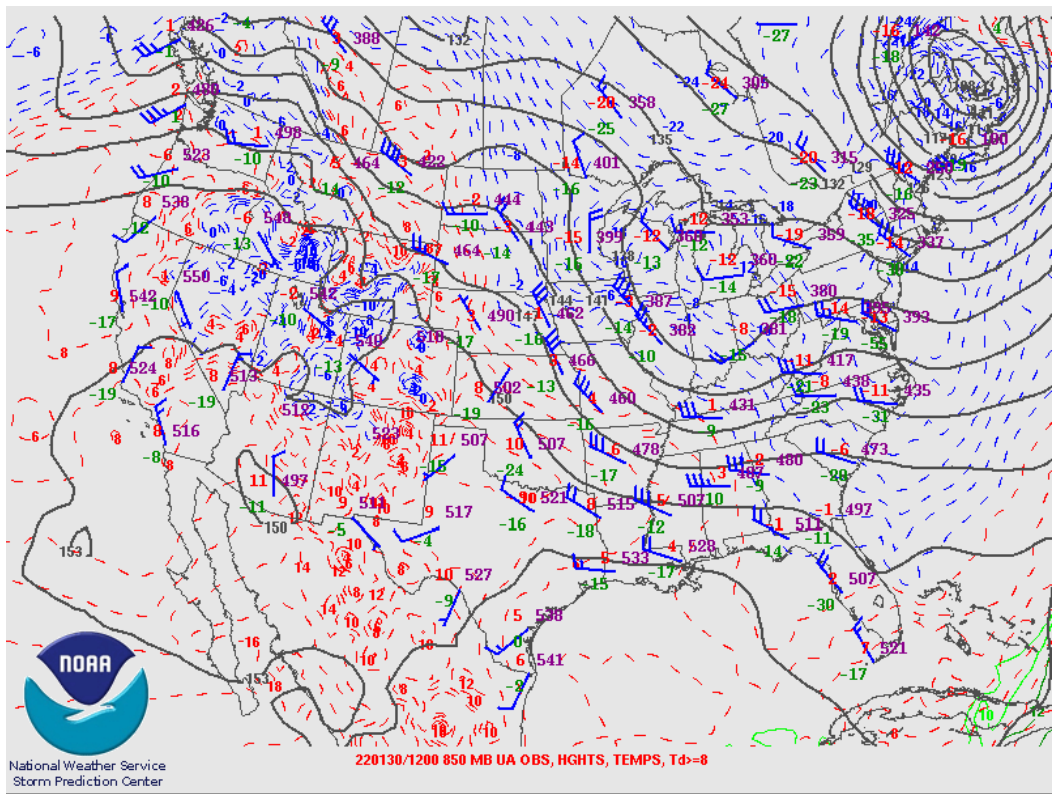


Figure 5. 850 mb Analysis for 7 AM Jan 30th (top), and 7 PM Jan 31st, 2022. Images obtained from <https://www.spc.noaa.gov/obswx/maps/>.

147 On January 30th, strong surface heating
 148 occurred at the surface following sunrise and
 149 was paired with the strong, deep inversion
 150 aloft. The surface heating initiated vertical
 151 thermal mixing near the surface, creating a
 152 shallow mixed layer. However, vertical
 153 plume movement was trapped by the deep
 154 inversion which is seen in the regional
 155 atmospheric soundings measured by the
 156 National Weather Service (Figure 6). The
 157 nearest sounding locations (identified in
 158 Figure 1) are located over 100 km away from
 159 the SRS, indicating that the inversion
 160 condition was a regional event occurring
 161 over several states in the region. Figure 6
 162 shows the morning and evening soundings
 163 or potential temperature profiles for January
 164 30th, 2022 at 0700 and 1900 LST where the
 165 increasing of potential temperature with height indicates a stable layer.

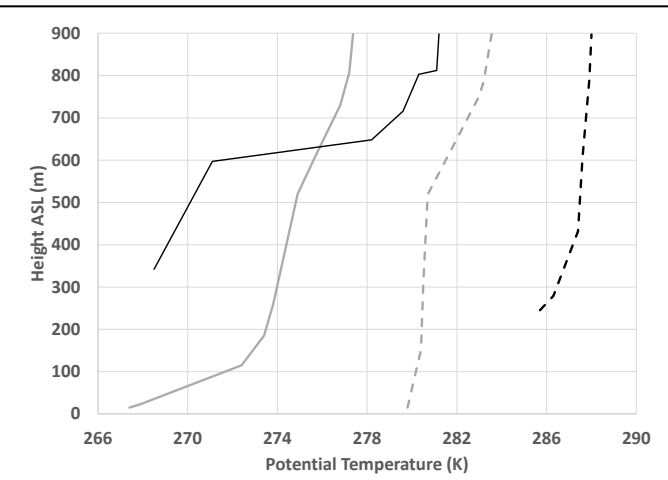


Figure 6: Potential temperature profiles from NWS soundings taken at the Peachtree City, GA (black) and Charleston, SC (gray) sounding sites identified in Figure 1 for 07:00 LST January 30th, 2022 (solid) and for 19:00 LST January 31st, 2022 (dashed).

166 Both temperature profiles indicate strong and deep stable layers that resulted from a combination of
 167 nocturnal cooling, cold air advection behind the cold front that passed through SRS the previous day,
 168 and the warm air advection aloft. Both Peachtree City and Charleston soundings have strongly stable
 169 layers through 500 m deep while all soundings were stable through the 900 m that was plotted, and
 170 remained stable throughout the entire day, indicating that thermal mixing was not sufficient to mix out
 171 the deep layer.

172 Examination of the SRS tower data showed an overnight low temperature of -7°C and is further

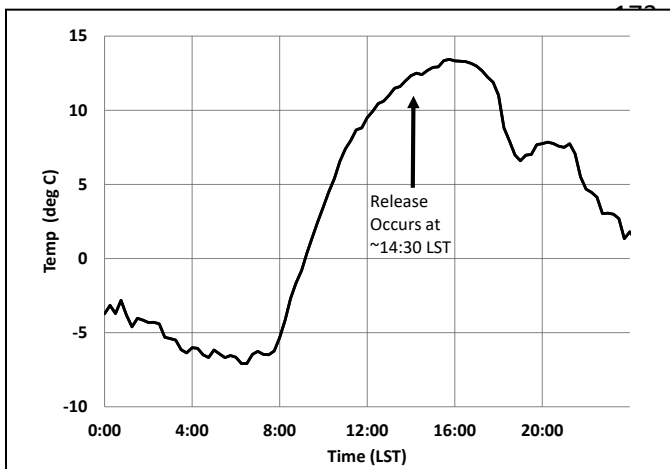


Figure 7. 2m temperature measurements from the SRS meteorological station on January 30, 2022.

173 indication of strong nocturnal cooling at the
 surface (Figure 7). After sunrise, the
 temperature increased rapidly, illustrative of
 the near-surface nocturnal inversion
 beginning to mix vertically by 0900 LST. SRS
 ceilometer data suggests that 1130 LST is
 approximately when the thermal mixing
 began to gradually deepen (Figure 8),
 followed by a more rapidly growing mixed
 layer beginning around 1330 LST. The release
 from the stack occurred after this point, at
 approximately 1430 LST. Despite occurring in
 afternoon, this was still early in the period of
 mixed layer growth for this day. The mixed

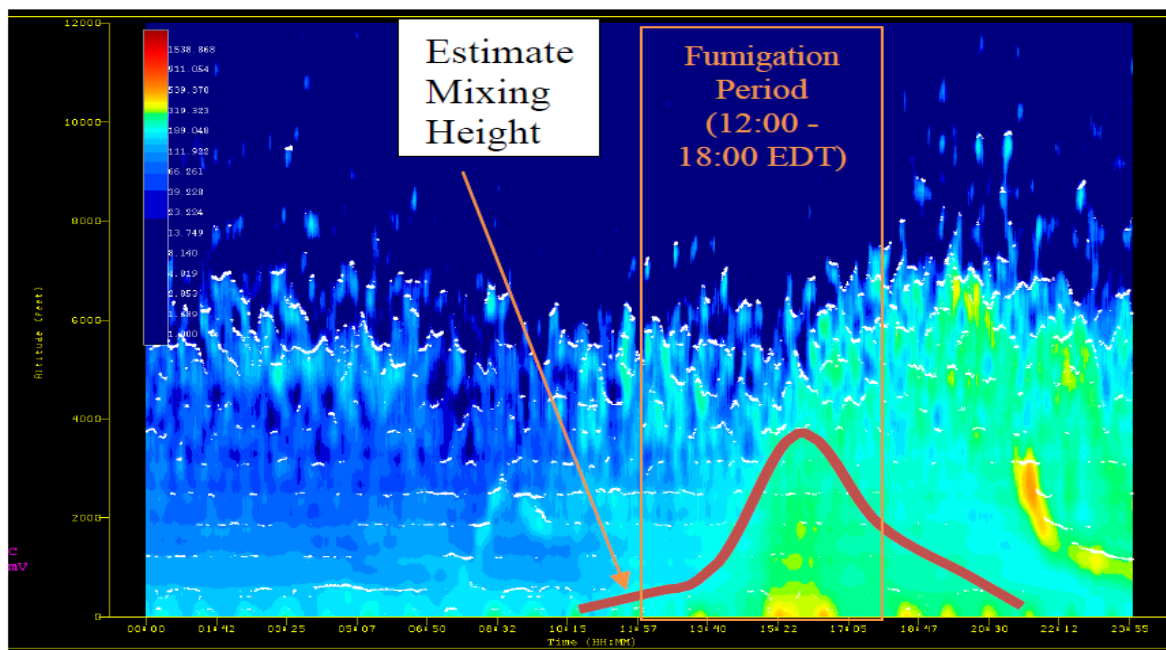


Figure 8. SRS Ceilometer data for January 30, 2022. Colors indicate “backscatter”, with the gradients in the colors suggesting where mixing is interrupted. Orange line indicates estimated mixing height. Uniform colors indicate more complete mixing.

187 layer height was approximately 500 m around this time, meaning that the strong thermal inversion was
 188 just starting to break. At this point, it is believed that the plume was still constrained to this depth and
 189 that downward mixing occurred as the thermal inversion was mixed out, leading to downward local
 190 motion of the plume that led to the plume being brought down to the surface.

191 An additional contributing factor is believed to be the wind speed, which had increased to around 4.5
 192 ms^{-1} beginning around 1130 LST (Figure 9). This is believed to be significant because stack-tip downwash
 193 is more pronounced at higher wind speeds and the increase in wind speed also causes more building
 194 induced wake turbulence. Wake models, such as AERMOD (US EPA 2019) or ARCON96 (Ramsdell et al.
 195 1997) usually produce the greatest concentrations with wind speeds of $2\text{-}4 \text{ ms}^{-1}$. Within these models,
 196 higher wind speeds generally lead to additional mechanical turbulence and dilution of the plume, while
 197 lower wind speeds typically do not produce enough turbulence to create a significant downwash effect.

198 *CFD Modeling for 30 January 2022*

199 The results of a 3 m s^{-1} reference velocity power law
 200 are shown in Figure 10. As can be seen in Figure 10a,
 201 the obstruction of the stack and the building on the
 202 right-hand side of the domain recirculates the air at
 203 the ground with a counter-circulation above it and
 204 an inflection point near the outlet. The results also
 205 show that the velocity profile higher in the
 206 atmosphere has a sudden increase in velocity
 207 followed by a decrease due to the recirculation.
 208 Figure 10b displays a closer view of the wind profile
 209 nearby the stack and buildings with wind
 210 recirculation occurring at multiple locations with an
 211 inflection point on the top of the building on the right. The obstruction of the stack with the wind profile
 212 approaching from left to right allows the wind to approach downward both near the buildings and the

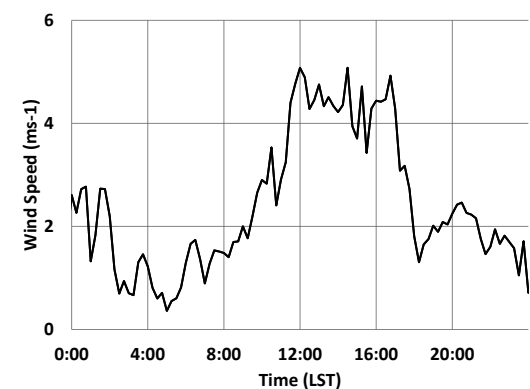


Figure 9. January 30th, 2022 18 m Wind Speed from CLM tower.

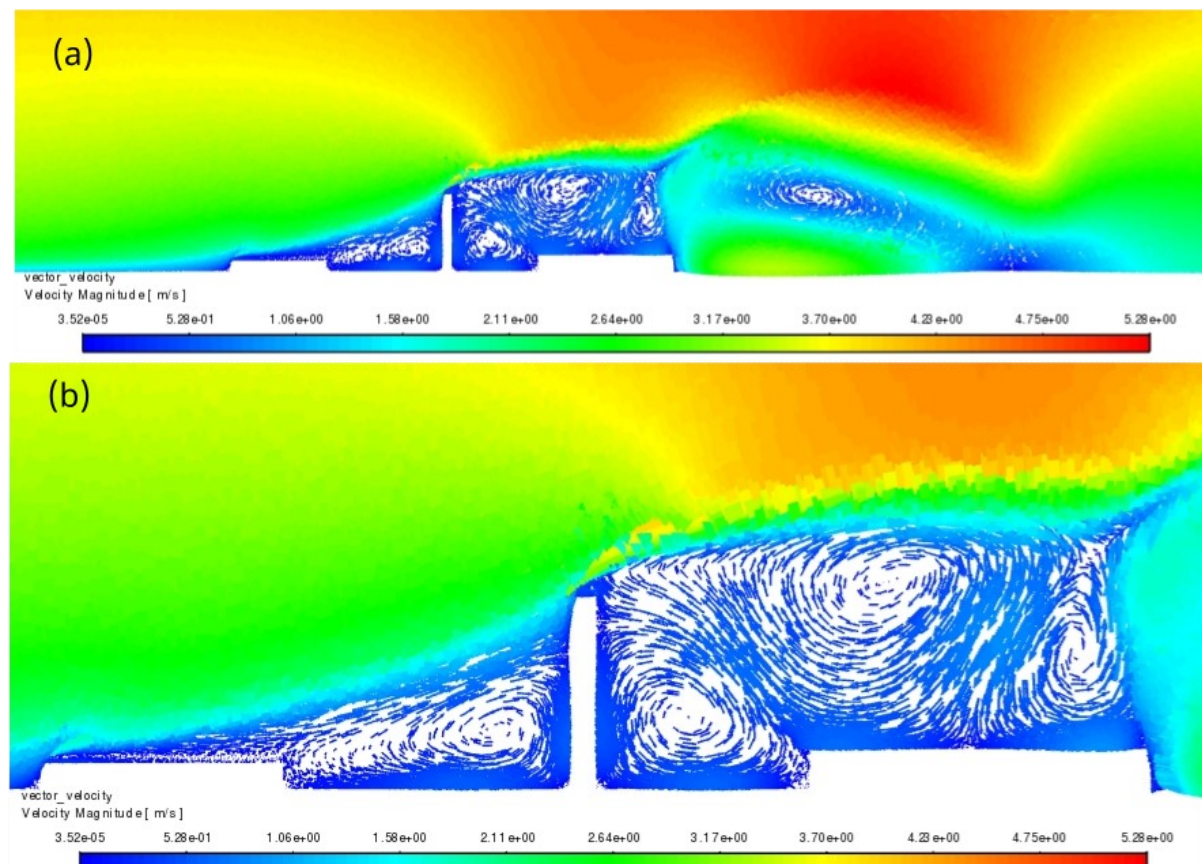


Figure 10. Wind velocity profile in (a) in the lower half of the domain and (b) close up of the stack and buildings.

213 ground. Therefore, this visualization of the downwash demonstrates it is possible that with the right
214 atmospheric conditions, a plume exiting the stack could possibly be trapped at the ground level and at
215 the top of either building, depending on the direction of the wind.

216 It should be mentioned that this is an initial step in developing more complex 2-D and/or 3-D studies of
217 the event. Future modeling of the event should include a detailed stack geometry in order to fully
218 capture stack downwash, as illustrated by Cain et al. (2003) when they simulated saturated buoyant
219 plumes with original, choke, and disk geometry designs at the stack exit. Further refinements may
220 include adaptive meshing to improve plume resolution as initial movement of the plume upon release
221 will depend on the outlet radius, as well as humidity of the air output from the stack and the ambient air
222 (Sivanandan et al., 2021, Cizek and Nozicka 2016). Therefore, more sophisticated simulation studies to
223 solve the Navier-Stokes equations would include realizable k-epsilon or large eddy simulations, in which
224 discrete meshing at building surfaces, the ground, and in the atmosphere with plume trajectories are
225 warranted and computational power would be high in demand. Finally, additional physics to condense
226 the plume would require some user defined functions as well as interpolating or extrapolating pressure,
227 temperature, and humidity at varying heights.

228

229 **Conclusions**

230 In this case, despite an elevated stack, it was found that surface concentrations were leading to
231 sufficient concentrations at the surface to cause alarm regarding uptakes for building air circulation
232 systems. The fact that this event happened in the afternoon during cool, clear conditions with moderate
233 wind speeds raises the question of the event's cause as most fumigation events which could lead to
234 high surface concentrations occur during stable or periods of transition from stable to unstable
235 conditions around or just after sunrise.

236 Fumigation events resulting from mixing of a near-surface thermal inversion typically occur in the
237 morning after sunrise as a result of an increase in surface sensible heat. The event which occurred on
238 January 30, 2022, is unusual in that the fumigation event occurred in the afternoon but appears to be
239 related to the presence of a strong thermal inversion which was not mixed out until afternoon. A key
240 factor in setting up these atmospheric conditions is the combination of strong surface radiational
241 cooling overnight from January 29 to January 30, with the advection of warm air into the region at
242 heights of approximately 1 km above the surface. This acted to create a much stronger inversion than
243 typically occurs in this region and required a longer period of time to mix out on the following day.

244 High-resolution modeling demonstrates that re-circulation is plausible based on input and boundary
245 meteorology conditions. The steady state of the boundary conditions will especially be important for
246 plume simulation at the specific time the safety alarms set off on January 30th. For the model itself,
247 additional physics such as heat exchanges, condensation modeling, and meteorological input data
248 should be carefully considered in future studies. Furthermore, a large meshing number should surround
249 the area of interest around the stack and the buildings to capture the turbulent boundary layer, and the
250 plume dynamics. When studying 3-D models, the stack exit may need to be more defined (lip, etc.) and

251 the building air intakes should be treated as sink sources (suck air into the facility). Finally, the turbulent
252 solvers for the event should be worked from realizable k-epsilon and Large Eddy Simulation studies, in
253 which, given their complex designs, will require large computational power for multiple runs.
254 Fortunately, a single event is necessary to study, but there might be additional events to evaluate. Once
255 when these events are studied, additional events seasonal to the SRS site will be simulated to warrant
256 any further action and prediction for worker safety such as redesigning the stack exit and/or cancel any
257 work during events where those specific conditions are observed.

258 Following an analysis of the event's cause, additional work will need to be pursued aimed at
259 understanding the likelihood of these events occurring in the future and whether surface dynamics such
260 as building downwash or local turbulence play a significant role. Unfortunately, studies developing a
261 climatology of strong inversion events such as the one described here have not been conducted based
262 on the perceived rarity of these events. Such an analysis could provide key data for understanding
263 whether events such as these need to be addressed in more detail for facility safety plans and identify
264 key atmospheric components or patterns that could be used to provide early warning for potential
265 impactful events stemming either from routine or unplanned releases.

266 **Funding**

267 This project was funded by the Savannah River Tritium Facility's Project Directed Research and
268 Development Program (Project SR23004).

269 **Acknowledgments**

270 The authors would like to acknowledge Marlene Moore and Kevin Cross for their assistance in
271 characterizing the details of the fumigation event.

272 This work was produced by Battelle Savannah River Alliance, LLC under Contract No.
273 89303321CEM000080 with the U.S. Department of Energy. Publisher acknowledges the U.S.
274 Government license to provide public access under the DOE Public Access Plan
275 (<http://energy.gov/downloads/doe-public-access-plan>).

276 **References**

277 Bierly, E. W. and Hewson, E. W., 1962: Some restrictive meteorological conditions to be considered in
278 the design of stacks. *Journal of Appl. Met.*, 1, 383-390.

279 Cain, Stuart A., Lewis A. Maroti, and Fangbiao Lin. "Prediction of Stack Plume Downwash Using
280 Computational Fluid Dynamics." *Fluids Engineering Division Summer Meeting*. Vol. 36967. 2003.

281 Cizek, Jan, and Jiri Nozicka. "Cooling tower plume." *AIP Conference Proceedings*. Vol. 1768. No. 1. AIP
282 Publishing LLC, 2016.

283 Feng, L., Yang, T., Wang, D., Wang, Z., Pan, Y., Matsui, I., ... & Huang, H. (2020). Identify the contribution
284 of elevated industrial plume to ground air quality by optical and machine learning methods.
285 *Environmental Research Communications*, 2(2), 021005.

286 Hossain, M., 2022: Fate and transport of stack emissions in the environment and potential reduction of
287 pollutants in the context of global warming. *J. Environmental Engineering*, 149,
288 doi.org/10.1061/(ASCE)EE.1943-7870.0002078.

289 Mushtaq, R., Bandh, S. A. and Shafi, S., 2020: Air pollution and its abatement. Chapter in *Environmental*
290 *Management*, Springer, 47-93.

291 Ramsdell, Jr., J. V., Simonen, C. A., Smyth, S. B., Lee, J. Y., 1997: Atmospheric relative concentrations in
292 building wakes. NUREG/CR-6331, Available online at
293 https://inis.iaea.org/collection/NCLCollectionStore/_Public/26/069/26069927.

294 Segal, M. and Pielke, R. A., 1983: On the evaluation of the mixing layer during elevated plume
295 fumigation. *J. Air Pollution Control Association*, 33, 1190-1192.

296 Sivanandan, Hrishikesh, et al. "A Study on Plume Dispersion Characteristics of Two Discrete Plume Stacks
297 for Negative Temperature Gradient Conditions." *Environmental Modeling & Assessment* 26.3 (2021):
298 405-422.

299 Warren, C. J., Paine, R. J., Connors, J. A., Szembek, C. and Knipping, E., 2022: Evaluation of a revised
300 AERMOD treatment of plume dispersion in the daytime elevated stable layer. *J. Air Waste Management*
301 Association, 72, doi.org/10.1080/10962247.2022.2094031.

302 Weinbeck, S.W., Viner, B.J. and A.M. Rivera-Giboyeaux, 2020: Meteorological Monitoring Program,
303 SRNL-TR-2020-00197, Savannah River National Lab, Aiken, SC, 138 pp. [Available online at
304 <https://weather.srs.gov/atg/static/pdf/SRNL-TR-2020-00197.pdf>]

305 U. S. Environmental Protection Agency, 2019: AERMOD: Model formation and evaluation. EPA-454/R-19-
306 014, 177pp.